

Predicting ripple roughness and sand resuspension under combined flows in a shoreface environment

Michael Z. Li ^a, L.D. Wright ^b, Carl L. Amos ^a

^a Geological Survey of Canada, Bedford Institute of Oceanography, Dartmouth, N.S. B2Y 4A2, Canada

^b Virginia Institute of Marine Science, College of William and Mary, Gloucester Point, VA 23062, USA

Received 6 May 1994; revision accepted 11 September 1995

Abstract

Ripple measurements and flow and sediment dynamical data obtained from the shoreface of the Middle Atlantic Bight using instrumented tripods were analyzed to evaluate various predictors of ripple geometry and roughness. Ripple roughness controls on sand resuspension and suspended sediment concentration profiles under combined waves and currents were also evaluated. The limited observation of sand ripples in the field indicates that the Grant and Madsen (1982) method overestimates ripple roughness, while the Nielsen (1981) method tends to under-predict ripple roughness. A modified ripple predictor is thus proposed based on the Grant and Madsen method, and it is shown to give reasonable predictions under the present experiment conditions.

This modified ripple prediction along with wave, current and suspended sediment concentration data recorded by the tripods were then brought into the combined-flow bottom boundary layer model of Grant and Madsen (1986) and the modified Rouse equation of Glenn and Grant (1987) to calculate sand resuspension coefficient γ_0 and to predict suspended sediment concentration profiles. It was found that under low-energy fair-weather conditions, sand ripples are in the equilibrium range and ripple roughness increases with the bed shear stress. This causes strong vortex activity close to seabed and thus higher resuspension coefficient. Reference concentrations are moderate due to this high resuspension coefficient, even though bed shear stresses are low. Under moderate storm conditions, ripple break off occurs and ripple roughness will decrease with bed shear stress. This reduces the vortex activity and hence sand resuspension coefficient γ_0 . The combination of this moderately high bed shear stress and reduced but still moderate ripple roughness favours sand suspension and produces the highest reference concentration for the encountered experimental conditions. As bed shear stress is further increased, ripples are nearly washed out and sand resuspension coefficient is further decreased approaching the previously-suggested constant value of 1.3×10^{-4} . This corresponds with the lowest reference concentration despite the high bed shear stress. Suspended sediment concentrations predicted by the modified Rouse equation using this time variable resuspension coefficient and properly calculated bottom boundary layer parameters are reasonable compared to the field measured concentration profiles.

1. Introduction

Several models have been developed to predict bed roughness, shear stress and velocity profiles in the bottom boundary layer (BBL) under combined wave-current flows over a movable bed (Smith,

1977; Grant and Madsen, 1979; Davies et al., 1988). All these models assume that the bottom roughness can be described by a single roughness scale k_b in which ripple roughness k_r is an important component. Studies have been conducted to understand ripple generation, stability, and their

effects on nearbed velocity and stress partitioning (Amos et al., 1988; Wiberg and Nelson, 1992; Li, 1994). Various models have been derived to predict ripple roughness for waves or combined flows (Nielsen, 1981; Grant and Madsen, 1982). However, these models are either based on laboratory data or for waves only, and have not been tested by combined-flow field data. Recent studies by Drake and Cacchione (1989), Vincent et al. (1991) and Vincent and Downing (1994) also indicate that ripple roughness, bed armouring and down-core increase of sediment cohesion can significantly affect the sediment resuspension coefficient γ_0 , which is critical in estimating the suspended sediment concentration (SSC) profiles. The values of γ_0 from these studies differ more than an order of magnitude, though they both show a systematic decrease in γ_0 with the increase of excess shear stress. This conflicts with the concept of constant γ_0 suggested by the flume experiments of Hill et al. (1988).

Several field experiments were conducted at the Virginia Institute of Marine Science (VIMS) during the period of 1985–1992 to observe bottom boundary layer dynamics and seabed responses in a shoreface environment. This paper is confined to data obtained in 1985 and 1988. Results obtained during a severe storm in 1991 were reported by Madsen et al. (1993). Detailed descriptions of these experiments, seabed responses to storms and cross-shore sediment transport have been given in Wright et al. (1986, 1991). In the present paper, limited combined-flow ripple measurements obtained from these experiments are used to evaluate the applicability of various ripple predictors to the combined flow conditions. The combined-flow bottom boundary layer model of Grant and Madsen (1979, 1986), as incorporated in a continental shelf sediment transport model SEDTRANS (Li and Amos, 1995), and a modified Rouse equation (Glenn and Grant, 1987) are used to calculate the bottom shear stress, reference concentration and sand resuspension coefficient under variable wave-current conditions. Correlations among these sediment and flow dynamical parameters are then analyzed to understand the bedform response to the change of wave-current

dynamics and how this controls sand resuspension and suspended sediment concentration profiles.

2. Experimental site and instrumentation

The data presented here were collected from the shoreface seaward of the U.S. Army Corps of Engineers Field Research Facility (FRF) at Duck, North Carolina (Fig. 1). The study site is located approximately halfway between Cape Hatteras in the south and the entrance to Chesapeake Bay in the north. The shoreface is concave upwards with a 0.6° upper shoreface (within 2 km from the shoreline) and a gentler lower shoreface of only 0.2° . The bottom sediment consists of well-sorted fine sand with a median grain size of 0.13 mm and a standard deviation of 0.29 mm. On the average sand composes 95.6% of the bottom sediment, silt and clay are only 2.3% and 2.1%, respectively. The annual average significant wave height at FRF is 0.9 m with an annual average peak spectral period of 8.7 s. Waves approach mainly from the south in the spring and summer, while winter storms generally come from the northeast. The coastal tides are semi-diurnal with a mean range of 1 m. Wind-driven currents are more important, and they typically flow southward alongshore. Details of the site can be found in Birkemeier et al. (1981).

The first experiment was conducted in September, 1985 at a depth of 8 m. The first five days were dominated by fair weather followed by storm conditions in the second half. The second experiment was conducted in January, 1988 at a depth of 7.3 m. High-energy swells dominated this experiment and were responsible for capsizing the instrument package after 20 hours of deployment. Time series of benthic oscillatory and net flows, fluctuating pressure, near bottom suspended sediment concentration profiles were measured using an instrumented tripod which is shown in Fig. 2. The instrumentation mainly consisted of four Marsh-McBirney electro-magnetic current meters, five miniature optical backscatter sensors (OBS), and a Paroscientific Digi-Quartz pressure sensor. The current meters were calibrated in steady flows before each deployment using a recirculating flume. OBS sensors were also calibrated using the

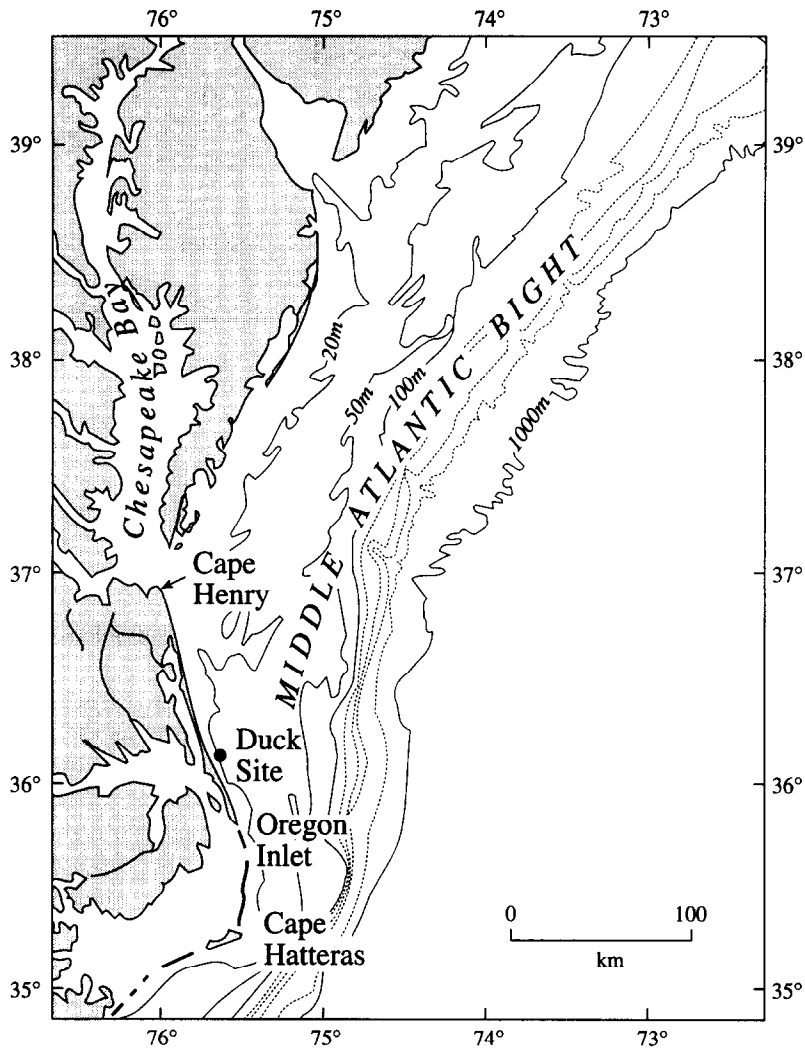


Fig. 1. Location map showing the experimental site Duck, North Carolina.

native bottom sediment collected from the field. All the sensors were synchronized and programmed for burst-mode sampling. The burst duration was 34 minutes for the 1985 experiment and 17 minutes for the 1988 deployment. The interval between bursts varied from 2 to 4 hours, and sampling frequency was set at 1 Hz. The tripod was deployed and retrieved by divers so that sensor orientation and elevations could be carefully observed. Ripple geometry and seabed roughness were examined by divers at the beginning, sometimes also at the end, of each deployment.

The raw data were analyzed to determine for each time series the water depth h , the significant wave height H_s , peak spectral wave period T , mean velocity u at the current sensor heights, the angle between waves and currents ϕ_{cw} and mean suspended sediment concentration at each height. These primary data are listed respectively in Table 1 for the 1985 fair weather, 1985 storm and 1988 high-energy swell conditions. The current meters at 20 cm height for the 1985 experiment and at 100 cm for the 1988 experiment gave the longest and most reliable records, thus their mean values were used in this study. The lowest mea-

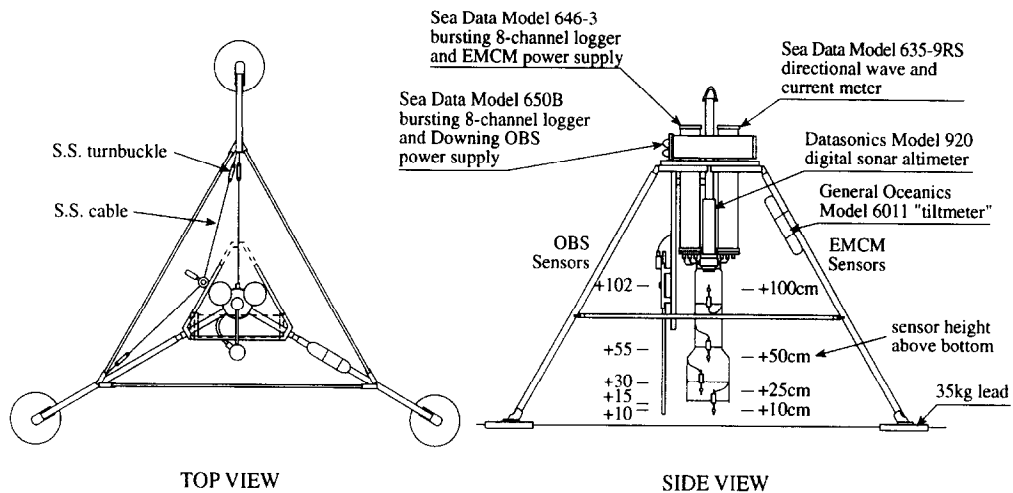


Fig. 2. The benthic boundary layer instrumented tripod used in this study.

sured suspended sediment concentration c_{z1} was at 14 cm and 10 cm above the seabed for the 1985 and 1988 experiments, respectively. The ripple height η and length λ observed by divers at the start of each deployment are also given in Table 1. Under continental shelf and nearshore environments, the non-linear interaction between waves and currents will enhance the BBL shear stresses. The widely-used combined-flow bottom boundary layer model of Grant and Madsen (1979, 1986, GM model hereafter) assumes a linear eddy viscosity function and utilizes the law of the wall velocity relationship to compute the various enhanced shear stresses and the velocity profiles above and below the wave boundary layer. Several field experiments have supported this model (Cacchione and Drake, 1982; Grant et al., 1984; Cacchione et al., 1987; Huntley and Hazen, 1988). The primary data in Table 1 were thus brought into the Grant and Madsen combined-flow bottom boundary layer model to calculate wave boundary layer thickness δ_w , bottom roughness z_0 , apparent bottom roughness z_{0c} , combined skin-friction shear velocity (u_{*cws}), and total wave (u_{*w}), current (u_{*c}) and combined wave-current (u_{*cw}) shear velocities. These parameters were then used in further analyses of the data. The essential BBL parameters obtained from the GM model are listed in Table 2 for the three experiments respectively.

3. Ripple roughness prediction

When flows exert force on a movable bed, ripples start to form as the friction on the seabed exceeds the threshold value for sediment movement. As waves and currents become stronger, ripples go through two distinct stages (Grant and Madsen, 1982). The first stage is known as the equilibrium range in which flow is relatively slow and sediment transport is low. Both ripple height η and ripple wave length λ tend to increase until ripple steepness η/λ and ripple roughness reach their maximum. Within the equilibrium range, the length of wave-formed ripples scales with the near bottom wave orbital excursion amplitude A_b . As flow strength is further increased, ripples enter the second stage defined as the break off range which involves strong flow and high sediment transport processes. When this break off point is reached, ripple height will decrease while ripple length stays roughly constant or decreases slightly. This will lead to the decrease in ripple steepness and ripple roughness, and also the de-correlation between wave excursion amplitude and ripple length. Many investigators have tried to quantitatively predict ripple height and length (Bagnold, 1946; Mogridge and Kamphuis, 1972; Miller and Komar, 1980a,b). However, the more popular ripple predictors are those of Nielsen (1981) and Grant and Madsen

Table 1
The field data for the Duck 1985 and 1988 experiments

Time (hour)	Depth (m)	H_s (cm)	Period (s)	u (cm/s)	ϕ_{cw} (degrees)	c_{z1} (mg/l)	η and λ (cm)
<i>1985 Fair Weather</i>							
2	8.73	41.9	10.1	1.3	14.2	824	$\eta = 3$ $\lambda = 15$
6	9.34	40.3	10.2	2.4	73.7	397	
10	9.22	42.9	10.8	0.5	80.4	723	
14	8.67	36.7	10.5	3.5	15.4	337	
18	9.06	28.3	9.9	1.4	3.8	153	
22	9.11	30.4	10.6	3.2	89.1	475	
26	8.68	29.7	10.7	1.1	64.7	265	
30	9.27	31.5	10.9	1.9	52.9	280	
34	9.43	28.2	10.7	2.4	83.6	401	
38	8.74	26.5	10.8	3.1	54.0	441	
42	8.94	24.0	11.1	2.2	48.1	451	
<i>1985 Storm</i>							
2	9.26	102.3	6.6	19.0	76.5	3064	$\eta = 2$ $\lambda = 20$
6	9.26	80.3	6.9	12.5	79.0	3852	
10	9.83	77.1	6.5	12.9	80.8	3204	
14	9.17	76.1	7.1	14.7	88.0	872	
18	9.15	73.6	7.0	7.4	81.5	1297	
22	9.99	86.0	8.3	8.7	85.5	1292	
26	9.35	87.7	8.1	12.6	88.3	2195	
30	9.01	86.2	7.0	8.6	87.0	2028	
34	9.89	84.3	6.8	15.4	85.5	1858	
38	9.45	99.4	6.6	35.0	73.2	1580	
42	9.12	125.1	6.7	24.0	78.2	1890	
<i>1988 Swell</i>							
1	6.52	89.2	9.6	3.1	76.7	589	$\eta = 1$ $\lambda = 10$
3	6.35	92.5	9.4	6.4	71.3	948	
5	6.60	94.4	9.4	9.3	77.7	655	
7	7.10	100.0	9.9	4.1	78.2	617	
9	7.21	101.7	10.1	1.6	27.7	773	
11	6.94	112.7	10.8	9.6	85.0	1530	
13	6.43	121.5	10.5	12.2	70.2	2350	
15	6.34	141.3	11.1	13.6	78.0	2035	
17	6.77	150.6	12.3	4.1	85.6	2003	

(1982, GM method hereafter). Wiberg and Harris (1994) compared these two methods with available wave ripple data and proposed a new ripple predictor. Though their method gave better prediction of ripples for the STRESS site on the northern California shelf, its overall performance was comparable to the Nielsen's (1981) method (Wiberg and Harris, 1994, p. 785). For their simplicity, the Nielsen method and the Grant and Madsen method only are further considered here.

Based on the laboratory data of Carstens et al. (1969), Grant and Madsen (1982) define the break

off skin friction Shields parameter as:

$$\theta_B = 1.8\theta_{cr}S_*^{0.6} \quad (1)$$

in which θ_{cr} is the sediment threshold Shields parameter and S_* is a dimensionless sediment parameter given by:

$$S_* = (D/4\nu)[(s-1)gD]^{0.5} \quad (2)$$

where D is the sediment diameter, ν is the kinematic viscosity, s is the specific gravity of sand (the ratio of sediment density ρ_s to the fluid density ρ), and g is the gravity acceleration. The ripple geometry

Table 2
Model output data for the 1985 and 1988 Duck experiments

Time (hour)	u_{*c} (cm/s)	u_{*cw} (cm/s)	u_{*cws} (cm/s)	δ_w (cm)	z_0 (cm)	z_{0c} (cm)	η (cm)	λ (cm)	S	c_0 (g/l)	γ_0
<i>1985 Fair Weather</i>											
2	0.47	5.33	1.40	6.84	0.56	5.65	3.0	15.1	0.48	4.49	0.00535
6	0.77	4.96	1.30	6.44	0.53	4.63	2.9	14.3	0.28	1.76	0.00355
10	0.22	5.34	1.38	7.31	0.60	6.70	3.2	16.2	0.44	8.78	0.01148
14	1.03	4.88	1.31	6.56	0.54	4.16	2.9	14.4	0.30	1.31	0.00253
<i>1985 Storm</i>											
2	2.71	6.64	2.74	5.57	0.13	1.21	1.5	19.8	4.68	17.04	0.00208
6	2.14	6.40	2.22	5.65	0.23	1.94	2.2	20.3	2.72	22.40	0.00469
10	2.23	6.43	1.99	5.33	0.32	2.00	2.5	18.5	1.98	16.78	0.00482
14	2.42	6.36	2.13	5.74	0.26	1.76	2.3	20.7	2.42	4.44	0.00105
18	1.50	6.33	2.03	5.62	0.28	2.76	2.4	20.1	2.12	10.18	0.00274
22	1.72	6.42	2.32	6.76	0.22	2.68	2.3	25.1	3.06	8.02	0.00149
26	2.17	6.43	2.45	6.60	0.18	1.96	2.0	24.6	3.53	12.31	0.00199
30	1.59	6.27	2.34	5.59	0.17	2.32	1.8	20.7	3.14	17.42	0.00316
34	2.46	6.37	2.18	5.52	0.24	1.64	2.2	19.8	2.58	9.76	0.00216
38	4.23	7.28	3.01	6.11	0.16	0.73	1.7	20.1	5.84	5.97	0.00058
42	3.25	7.40	3.33	6.31	0.10	1.04	1.0	20.8	7.38	8.68	0.00067
<i>1988 Swell</i>											
1	0.46	7.10	3.10	8.65	0.13	6.59	1.5	31.1	6.25	3.35	0.000305
3	0.87	7.35	3.26	8.74	0.12	5.26	1.4	30.5	7.03	3.86	0.000313
5	1.19	7.34	3.26	8.82	0.12	4.40	1.4	30.8	7.03	2.43	0.000197
7	0.60	7.40	3.28	9.32	0.12	6.55	1.4	32.5	7.13	2.35	0.000188
9	0.26	7.44	3.30	9.56	0.12	8.23	1.5	33.3	7.25	3.28	0.000257
11	1.32	8.23	3.71	11.30	0.13	5.50	1.3	36.6	9.38	4.19	0.000254
13	1.68	9.29	4.17	12.42	0.14	5.51	1.0	36.1	12.14	5.64	0.000265
15	2.02	10.97	4.77	15.54	0.18	6.80	0.8	39.3	16.19	4.10	0.000144
17	0.79	11.14	4.83	17.50	0.19	12.66	0.9	44.2	16.62	3.96	0.000136

is predicted for both the equilibrium and break-off ranges. The maximum skin-friction wave Shields parameter, θ_{wm} , can be defined:

$$\theta_{wm} = \rho u_{*wm}^2 / (\rho_s - \rho) g D \quad (3)$$

in which u_{*wm} is the maximum skin-friction wave shear velocity predicted by the GM model using a grain roughness $2.5D$. For ripples in the equilibrium range, $\theta_{wm} < \theta_B$:

$$\eta = 0.22 A_b (\theta_{wm} / \theta_{cr})^{-0.16} \quad (4a)$$

$$\lambda = 6.25 \eta (\theta_{wm} / \theta_{cr})^{0.04} \quad (4b)$$

For ripples in the break-off range, $\theta_{wm} > \theta_B$:

$$\eta = 0.48 A_b (\theta_{wm} / \theta_{cr})^{-1.5} \quad (5a)$$

$$\lambda = 3.6 \eta S_*^{-0.6} (\theta_{wm} / \theta_{cr}) \quad (5b)$$

The ripple predictor of Grant and Madsen (1982) is based on the wave-tank data of Carstens et al. (1969). Nielsen (1981) suggests that natural ripples are shorter and less steep due to the irregularity of natural waves. Based on wave-ripple field data of Inman (1957) and Dingler (1974), he obtained the following field wave-ripple predictor:

$$\eta = 21 A_b M^{-1.85} \quad M > 10 \quad (6)$$

$$\eta / \lambda = 0.342 - 0.34 \theta_{wm}^{0.25} \quad (7)$$

where the wave-mobility number M is defined as:

$$M = u_b^2 / (s - 1) g D \quad (8)$$

in which u_b is the near-bed wave orbital velocity.

Once the ripple height and ripple wave length are obtained, the following method of Grant and

Madsen (1982) is adopted for the prediction of ripple roughness, K_r , in this study:

$$K_r = 27.7\eta(\eta/\lambda) \quad (9)$$

Time series of ripple height, ripple wave length and ripple roughness predicted by various models, including a modified Grant and Madsen method, are compared in Fig. 3 for the 1985 Duck fair-weather period. Similar comparisons are shown in Figs. 4 and 5 for the 1985 storm period and 1988 swell condition respectively. Normalized excess

shear stress S (see definition below) was also shown in the bottom plot in each figure. For the 1985 fair-weather experiment, the measured ripple height and length at the beginning of the experiment were 3 cm and 15 cm respectively (Table 1). This produces a ripple roughness of 16.6 cm from Eq. 9. Fig. 3 shows that under fair-weather conditions, the GM method generally over-predicts ripple height, ripple length and ripple roughness compared to the measured data. Though the Nielsen method predicts reasonable values, it sug-

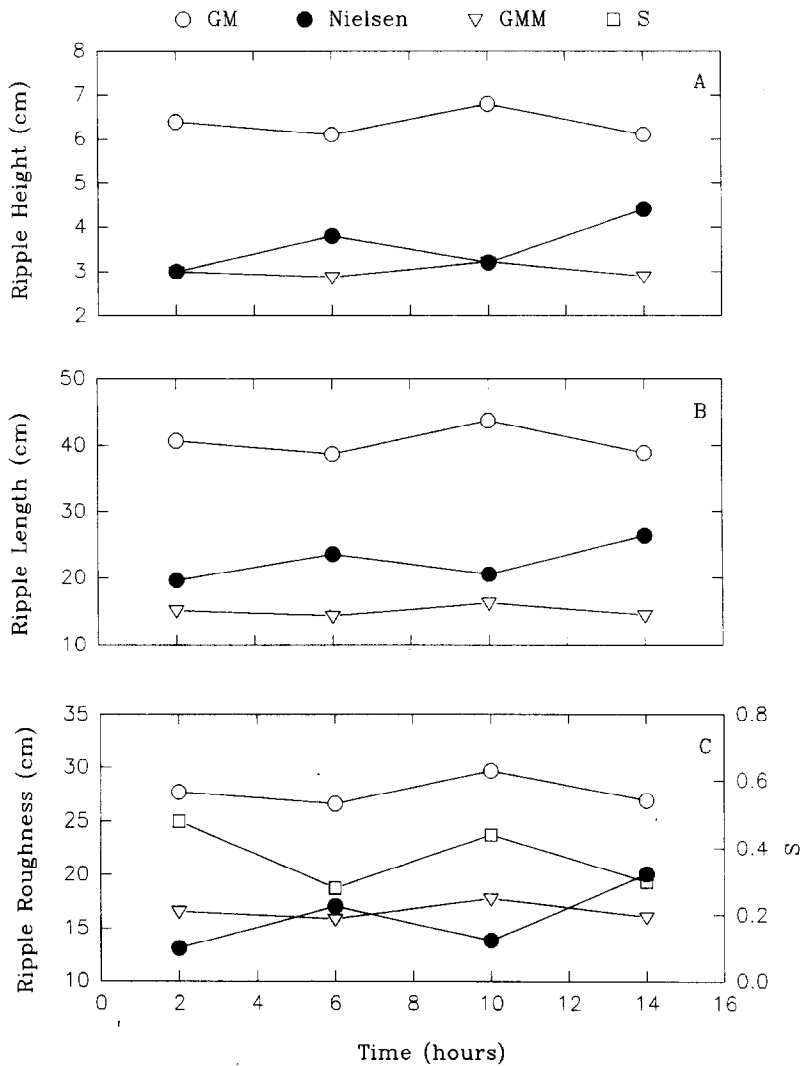


Fig. 3. Time series of model-predicted ripple height (A), ripple length (B), ripple roughness and excess shear stress S (C) for the 1985 fairweather period. Circles, Grant and Madsen (1982); dots, Nielsen (1981); triangles, modified Grant and Madsen method; squares, excess shear stress.

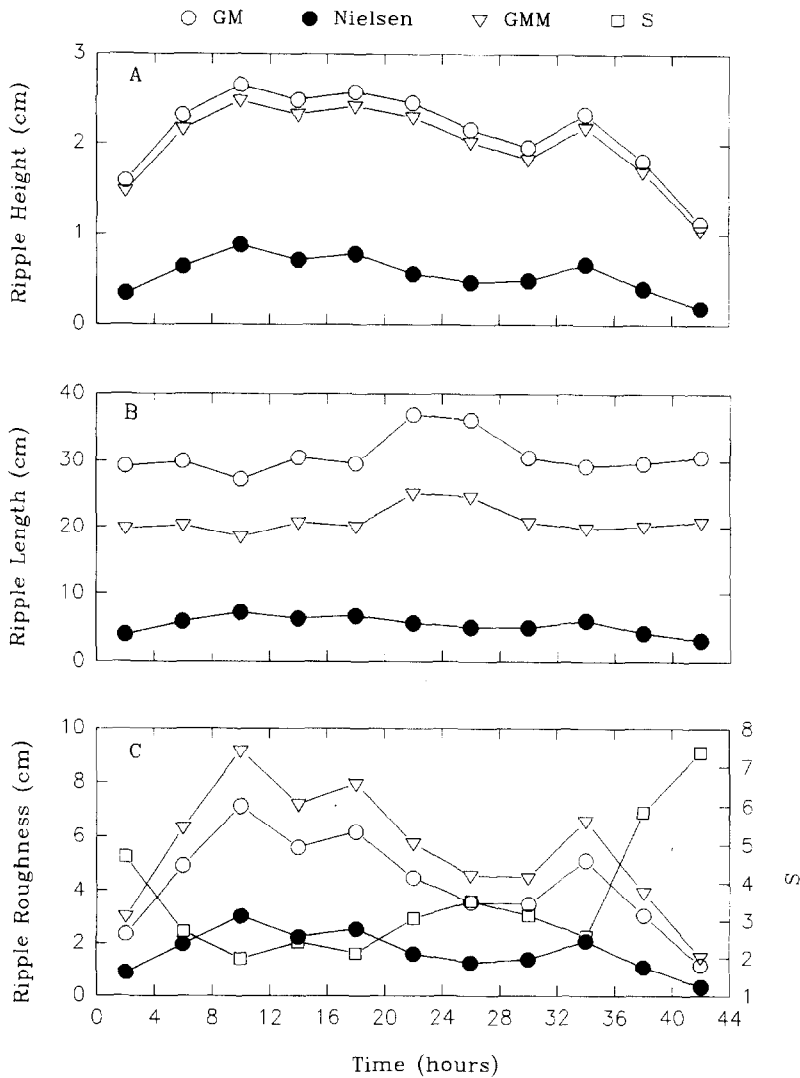


Fig. 4. Time series of model-predicted ripple height (A), ripple length (B), ripple roughness and excess shear stress S (C) for the 1985 storm period. Symbols are defined as in Fig. 3.

gests decreasing ripple height and ripple roughness with the increase in bed shear velocity, which is opposite to the concept of increasing ripple height and roughness with stronger bed shear stress under the equilibrium condition. The measured ripple height and length are 2 cm and 20 cm respectively for the 1985 storm period. These correspond with a ripple roughness of 5.5 cm. Fig. 4 shows that the GM method gives good prediction of ripple height, though the ripple length is over-predicted. In contrast to the fair-weather condition, Nielsen's

method generally under-predicts all ripple parameters under the storm condition. Based on the 1985 Duck experiment data and arguments of Cacchione and Drake (1990), an iterative trial-and-error method was used to obtain the following modified Grant and Madsen ripple predictor: for $\theta_{wm} < \theta_B$,

$$\eta = 0.101 A_b (\theta_{wm} / \theta_{cr})^{-0.16} \tag{10a}$$

$$\lambda = 4.95 \eta (\theta_{wm} / \theta_{cr})^{0.04} \tag{10b}$$

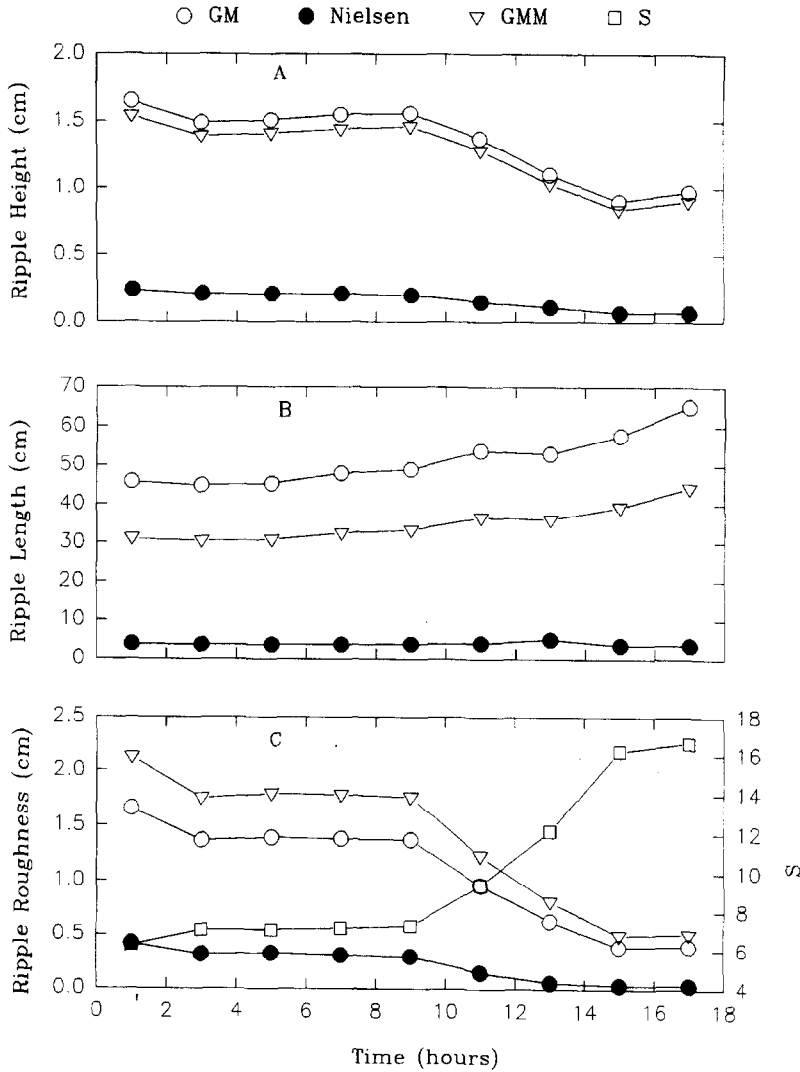


Fig. 5. Time series of model-predicted ripple height (A), ripple length (B), ripple roughness and excess shear stress S (C) for the 1988 experiment. Symbols are defined as in Fig. 3.

for $\theta_{wm} > \theta_B$:

$$\eta = 0.356 A_b (\theta_{wm} / \theta_{cr})^{-1.5} \tag{11a}$$

$$\lambda = 3.03 \eta S_*^{-0.6} (\theta_{wm} / \theta_{cr}) \tag{11b}$$

The ripple parameters predicted by this modified Grant and Madsen method are also shown in Figs. 3 and 4. They are in good agreement with the field measurements for the Duck 1985 experiments.

Ripple parameters predicted by the GM method, the modified GM method and the Nielsen method

are compared in Fig. 5 for the Duck 1988 experiment. For this experiment period, the ripple height measured at the start of the experiment was 1 cm and ripple length was 10 cm (Table 1). These values give a ripple roughness of 2.8 cm. Fig. 5 shows that under this high-energy swell condition, ripple height and ripple roughness are reasonably predicted by the GM and modified GM methods, though ripple length is over-predicted by both methods. Nielsen method again significantly under-predicts all ripple parameters. Although the

modified GM ripple predictor overestimates ripple wave length for the 1988 experiment (Fig. 5B), the predicted ripple roughness is reasonable compared to the measured ripple roughness. Also further change of Eq. 11 according to the 1988 data will significantly under-predict ripple length for the 1985 experiments. Thus Eq. 11 is not further modified to fit the 1988 data.

The ripple geometry was not measured for each sampling burst, but rather limited to the beginning and/or the end of each deployment in the Duck experiments. Ripple roughness would not change significantly for the fair-weather period, but it should have decreased with the increasing bed shear stress in the storm and swell conditions. This limitation was overcome in a similar field experiment conducted on the Scotian shelf at Bedford Institute of Oceanography (Li et al., 1993). The temporal variation of measured ripple roughness is compared with the predictions by various models in Fig. 6 for selected bursts from this experiment. It clearly demonstrates that the original GM method strongly over-predicts ripple roughness, while the applicability of the Nielsen method is uncertain. For some bursts of strong current dominance over waves, the Nielsen method predicts no ripple formation, though the field measurements

show sediment transport and ripple development. In contrast, the modified GM method again gives the best prediction. A detailed description of the Scotian shelf experiment and final modification of the GM ripple predictor will be presented in a separate publication. The modified GM method given in Eqs. 10 and 11 together with the GM boundary layer model are used here for the predictions of ripple height, length and BBL parameters (Table 2). These are then used in sand resuspension analyses in this paper.

4. Sand resuspension

Based on the Rouse (1937) concentration equation for unidirectional flows, the vertical distribution of suspended sediment concentration under combined waves and currents can be calculated using the following modified Rouse equations (Glenn and Grant, 1987):

$$C_z = C_{\delta_w}(z/\delta_w)^{-\alpha} \text{ for } z > \delta_w \quad (12a)$$

$$C_z = C_0(z/z_0)^{-\alpha} \text{ for } z < \delta_w \quad (12b)$$

where C_z is the mean suspended sediment concentration at height z above the seabed, C_{δ_w} is the

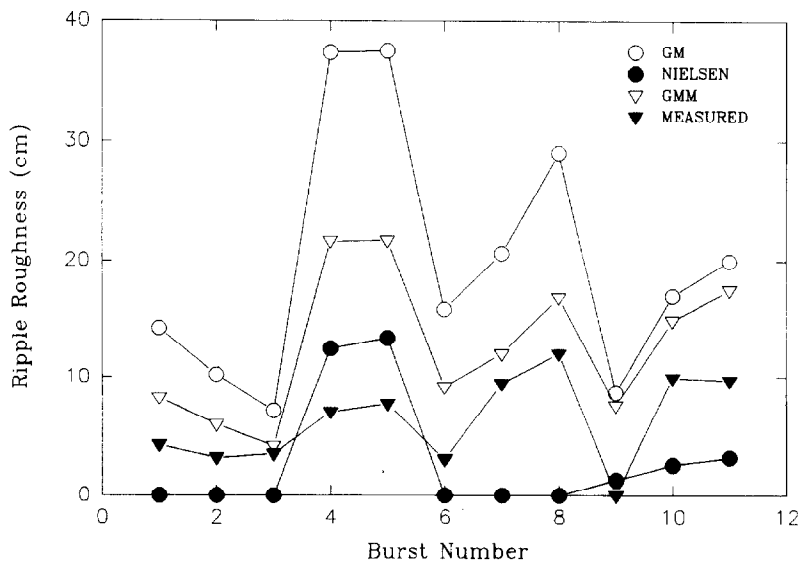


Fig. 6. Time series of measured and predicted ripple roughness for selected bursts from the Scotian shelf experiment. Solid triangle represents the measured ripple roughness and other symbols are defined as in Fig. 3.

mean SSC at the top of the wave boundary layer, C_0 is the reference concentration at the height of the bottom roughness z_0 , and α is the suspension parameter:

$$\alpha = \gamma w_{s1} / \kappa u_{*c} \quad \text{for } z > \delta_w$$

$$\alpha = \gamma w_{s2} / \kappa u_{*cw} \quad \text{for } z < \delta_w$$

in which γ is an empirical constant set to 0.74 according to Businger et al. (1971), w_{s1} and w_{s2} are sediment grain settling velocities above and below the wave boundary layer, respectively. Based on the work of Smith and McLean (1977), a simplified method is used here for the computation of reference concentration C_0 :

$$C_0 = C_b \gamma_0 S \quad (13)$$

where $C_b = 0.65$ is the volume concentration of sediment in the bed, S is the normalized excess shear stress defined as $(\tau' - \tau_{cr}) / \tau_{cr}$ with τ' being the skin friction shear stress and τ_{cr} the critical shear stress for sediment initiation of motion, and γ_0 is the so-called sediment resuspension coefficient representing the relative efficiency of sand resuspension.

In order to compute sediment concentration using the above-described method, the fall velocities above and below the wave boundary layer, w_{s1} and w_{s2} , must be known. Vertical grain size distribution was not measured in the Duck experiments. Thus we can not obtain the actual values for w_{s1} and w_{s2} . It is well established, however, that the ratio of shear velocity to settling velocity has to be equal to or larger than 1 for suspension to occur. Based on the model-predicted total current and combined shear velocities u_{*c} and u_{*cw} listed in Table 2, the settling velocities are assumed to be 1.05 cm/s (the settling velocity for $D_{50} = 0.13$ mm) for all the experiments except the 1985 fair-weather period, in which $w_{s1} = 0.25$ cm/s has been taken because of the low current shear velocity (averaging only 0.5 cm/s). After the settling velocities are defined, the measured suspended sediment concentration at the lowest height above the seabed (c_{z1} in Table 1) and corresponding BBL parameters from the GM model based on the modified ripple predictor are brought into Eq. 12a to calculate C_{δ_w} which is then inserted in Eq. 12b for the computa-

tion of C_0 at the height of the wave boundary layer bottom roughness z_0 . This reference concentration and proper shear stresses are then used in Eq. 13 to obtain the resuspension coefficient γ_0 . The values of S , C_0 and γ_0 computed this way are also listed in Table 2 for each burst. Since u_{*cws} is below the critical shear velocity $u_{*cr} = 1.15$ cm/s for hours 18 to 42 in the 1985 fair-weather experiment, no calculations are performed for these bursts.

Time series of resuspension coefficient γ_0 and reference concentration C_0 are plotted in Fig. 7B for the 1985 fair-weather condition. Temporal variation of normalized excess shear stress S and model-predicted ripple roughness K_r are shown in Fig. 7A in comparison to understand the control of bedform development on sand resuspension. Similar plots are also given in Figs. 8 and 9 for the 1985 storm and 1988 swell conditions, respectively. Fig. 7 suggests that under the fair-weather condition, the combined skin-friction shear velocities (u_{*cws} in Table 2) are smaller than the ripple breakoff shear velocity 1.61 cm/s given by Eq. 1 and sand ripples are still in equilibrium range, thus ripple roughness increases with the increase in bed shear stress. This increased ripple roughness then leads to stronger vortex activity close to seabed, hence higher sand resuspension coefficient and reference concentration at the height of z_0 (Fig. 7B).

Ripple development and sand resuspension under storm conditions are quite different than that for the low-energy fair-weather conditions. Combined shear velocities for the 1985 storm period are moderately above the ripple break off limit (Table 2) and sand ripples are in the break off range. Time series of S , K_r , γ_0 and C_0 plotted in Fig. 8 generally show that the increase in normalized excess shear stress S causes decreasing ripple roughness under this condition. This decrease in ripple roughness then causes reduced vortex ejection of sands, decreased sand resuspension coefficient γ_0 and suspended sediment concentration at z_0 , though the average values of C_0 are higher than that under the fair-weather condition (Fig. 7B). For the 1988 high energy swell condition, the values of S are as high as 16 and u_{*cws} are significantly higher than the break off value of

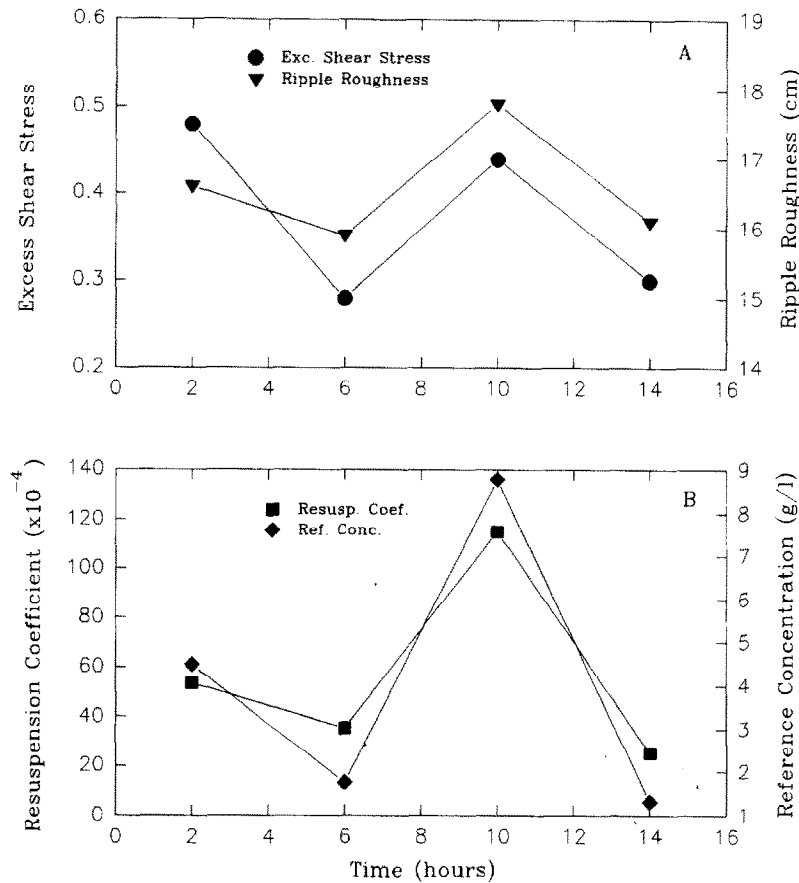


Fig. 7. Time series of (A) excess shear stress and ripple roughness, and (B) resuspension coefficient and reference concentration for the 1985 fairweather period.

1.61 cm/s (see Table 2). Under this energetic condition, ripple roughness again decreases with the increasing bed shear stress and this, among other factors such as bed armouring, leads to a general decrease in the sand resuspension coefficient γ_0 (Fig. 9B). In contrast to the low to medium energy conditions of 1985 experiment, the reference concentration of the 1988 experiment generally shows an increasing trend with the increase of bed shear stress for the first three quarters of the deployment period (from hours 1 to 13 in Fig. 9B), despite the decrease in ripple roughness K_r and sand resuspension coefficient γ_0 during this period. From hours 13 to 17, C_0 again shows the same positive correlation with ripple roughness and resuspension coefficient, dramatically decreasing with the decrease of K_r and γ_0 .

The three experiments can be compared as individual events of different energy levels. The normalized excess shear stresses are less than 1 in the 1985 fair-weather event and increase to moderate values of 2 to 8 for the 1985 storm period and to very high values between 6 to 18 in the 1988 swell event. With this increase in bed shear stress, the average ripple roughness systematically decreases from 16.6 to 5.5 and 1.4, respectively. This then corresponds with a decrease in the average resuspension coefficient from 0.0057 to 0.0023 and 0.00020, respectively. Though bed shear stresses are low under the 1985 fair-weather condition, reference concentrations still reach moderate values due to higher ripple roughness and efficient sand resuspension (the average C_0 is equal to 4.08 g/l). Despite the decrease in ripple roughness

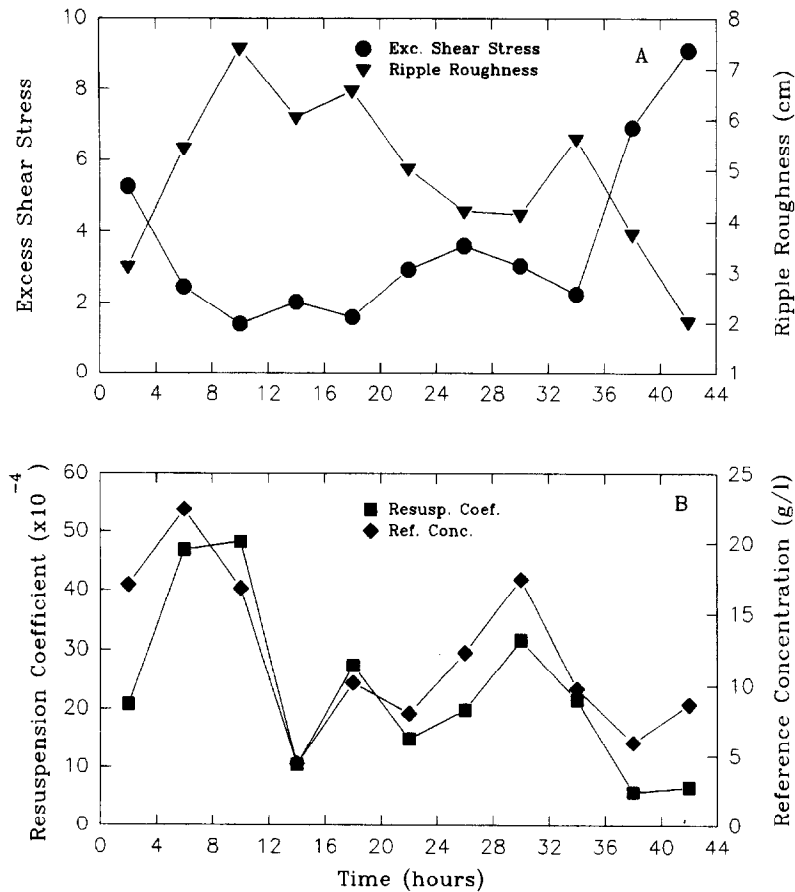


Fig. 8. Time series of (A) excess shear stress and ripple roughness, and (B) resuspension coefficient and reference concentration for the 1985 storm period.

and resuspension coefficient during the 1985 storm period, the increase in bed shear stress is more important and has led to a strong increase in C_0 with the average concentration reaching 12.1 g/l. As bed shear stress is further increased for the 1988 swell condition, the seabed is nearly flat and an armouring layer may have developed. This dramatically reduces sand resuspension and the average reference concentration is the lowest, being only 3.68 g/l.

Various authors have suggested different values of γ_0 ranging from 1×10^{-2} to 1.5×10^{-5} (Smith and McLean, 1977; Wiberg and Smith, 1983; Kachel and Smith, 1986). Unidirectional flume experiments by Hill et al. (1988) suggest that this wide spread of estimated γ_0 values could be due to measurement errors and/or uncontrolled vari-

ables, and thus a constant value of 1.3×10^{-4} should be used. Recent field studies by Drake and Cacchione (1989) on mud, and by Vincent et al. (1991) and Vincent and Downing (1994) on sand, however, show that γ_0 systematically decreases with the excess shear stress, though the causes of this decrease and the magnitudes of their estimates are different. The data of Vincent et al. for sands are mainly in the ripple break off range and thus it is unknown how γ_0 (hence sand resuspension) reacts to boundary dynamics when ripples are still developing in the equilibrium range. The logarithmic values of γ_0 are plotted in Fig. 10 against the logarithmic values of S for data from all three Duck experiments. Data of Vincent et al. (1991) are also included for comparison. Good agreement between our data and that of Vincent et al. is

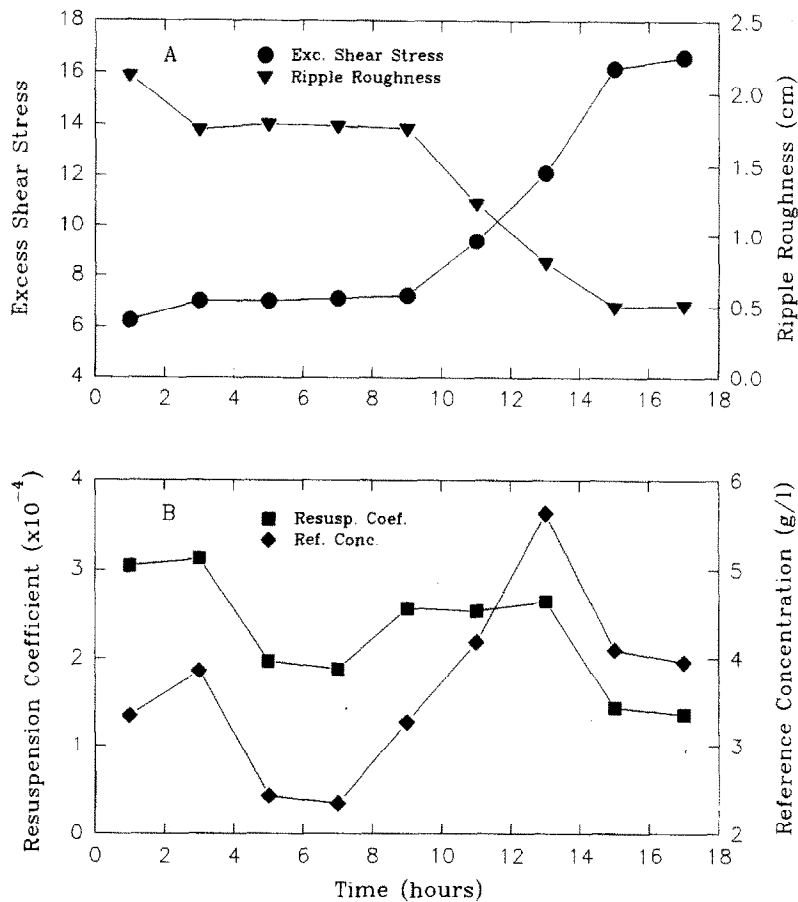


Fig. 9. Time series of (A) excess shear stress and ripple roughness, and (B) resuspension coefficient and reference concentration for the 1988 experiment.

found. The combined data from these two studies clearly indicate that sand resuspension coefficient γ_0 is not a constant and its value should decrease with the increasing bed shear stress in the ripple break off range. In the equilibrium range, however, our data show that γ_0 will increase with the bed shear stress. This segmented data pattern thus implies that most efficient sand resuspension should occur for moderate bed shear stress and well-developed sand ripples around the break-off point. Linear regression of the two data groups in Fig. 10 has resulted in the following empirical relationships for the prediction of γ_0 under combined flows:

$$\gamma_0 = 0.0355S^{1.94} \quad r^2 = 0.70 \quad \text{for } S < 1 \quad (14a)$$

$$\gamma_0 = 0.0206S^{-1.93} \quad r^2 = 0.85 \quad \text{for } S > 1 \quad (14b)$$

5. Predicting sediment suspension profiles

The Rouse equation for suspended sediment concentration profiles, given in a simplified version in Eq. 12, has been widely used by oceanographers, all though it has not been well tested in the sea (Sternberg et al., 1986). The biggest difficulty in applying the Rouse equation is the specification of c_0 based on Eq. 13 in which c_0 is related to the excess shear stress S through the resuspension coefficient γ_0 . There is no agreed universal selection of the height for c_0 , and values of γ_0 from various studies can be different more than 2 or 3 orders of magnitude. Theoretical modelling has been done (Smith, 1977; Smith and McLean, 1977) and techniques have been suggested in using the Rouse equation for marine boundary layers (McCave,

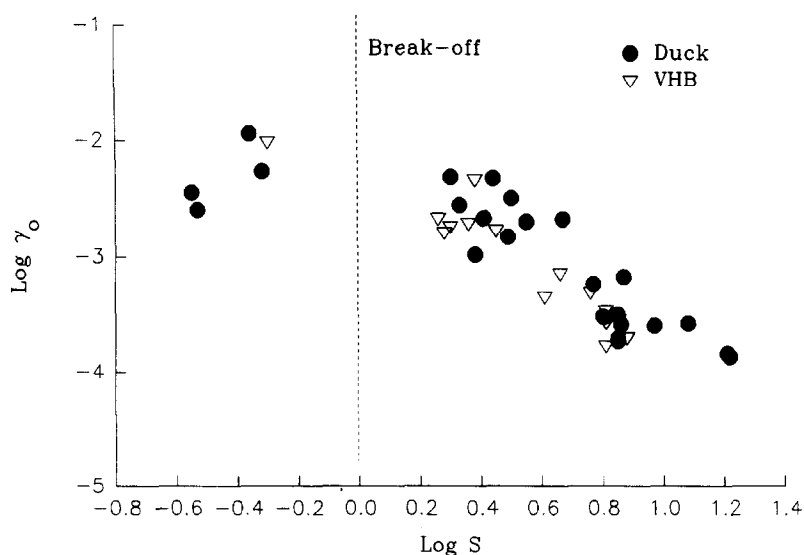


Fig. 10. Variation of sand resuspension coefficient γ_0 with excess shear stress S for this study (circles) and Vincent et al. (1991, triangles). Break off value is shown by the dashed line.

1973; Adams and Weatherly, 1981; Vincent et al., 1982). Nielsen (1984) has also compared measured suspended sediment concentration profiles under waves with the predictions by a similar exponential-decay equation. Only a few attempts have been made to model SSC profiles under combined waves and currents (Vincent and Green, 1990; Vincent et al., 1991), and these have generally shown that the predicted concentrations are an order of magnitude different from the measured concentrations. An exception is the recent work of Wiberg et al. (1994). By considering the effects of bed armouring and suspension stratification, they found good agreement between predicted and measured light attenuation values at two heights. In light of the modified ripple predictor (Eqs. 10 and 11) and empirical γ_0 function of Eq. 14, the Duck experiments provide an excellent set of data to test the applicability of the Rouse equation under combined waves and currents for conditions ranging from low energy fair weather to high-energy storm and swell situations.

Recent flume experiments by Hill et al. (1988) suggests that the resuspension coefficient γ_0 should be a constant of 1.3×10^{-4} . But field measurements by Drake and Cacchione (1989), Vincent et al. (1991) and this study (Fig. 10) all show that γ_0

can be affected by bed armouring, changing ripple roughness and increasing cohesion at depth in the substrate. A constant γ_0 of 1.3×10^{-4} and appropriate BBL parameters are used in Eqs. 12 and 13 to calculate suspended sediment concentrations for the 1985 and 1988 experiments, respectively. Time series of these model-predicted concentrations are plotted in Fig. 11 against the measured concentrations at selected heights for all three experiments. This comparison shows that using the constant γ_0 of 1.3×10^{-4} underestimates the suspended sediment concentration by more than one order of magnitude for the 1985 fair-weather experiment and for most bursts of the 1985 storm experiment. Better agreement is found towards the end of the 1985 storm experiment and for the 1988 swell condition since $\gamma_0 = 1.3 \times 10^{-4}$ is reasonably close to the estimated γ_0 based on measured sediment concentrations under these energetic conditions. Even in the 1988 high-energy swell conditions, differences of an order of magnitude are found between the measured and model predicted concentrations at upper heights (20 and 50 cm) for some of the bursts (Fig. 11C). This large discrepancy between measured and model predicted SSC profiles indicates that a constant γ_0 of 1.3×10^{-4} generally under-predicts suspended

sediment concentration by an order of magnitude for the low to moderately high energy conditions and thus can not be used in predicting suspension profiles under the combined wave and current flows in shoreface environments.

In contrast, we have used the empirical γ_0 relationships given in Eq. 14 to calculate γ_0 based on the skin friction excess shear stress S . This variable

γ_0 , together with the BBL parameters calculated from the GM model using the modified ripple predictor given in Eqs. 10 and 11, is then used in Eqs. 13 and 12 to recalculate the suspension profiles for all three Duck experiments. Time series of these recalculated concentrations are plotted in Fig. 12 against the measured concentrations at the same corresponding heights as those shown in Fig. 11.

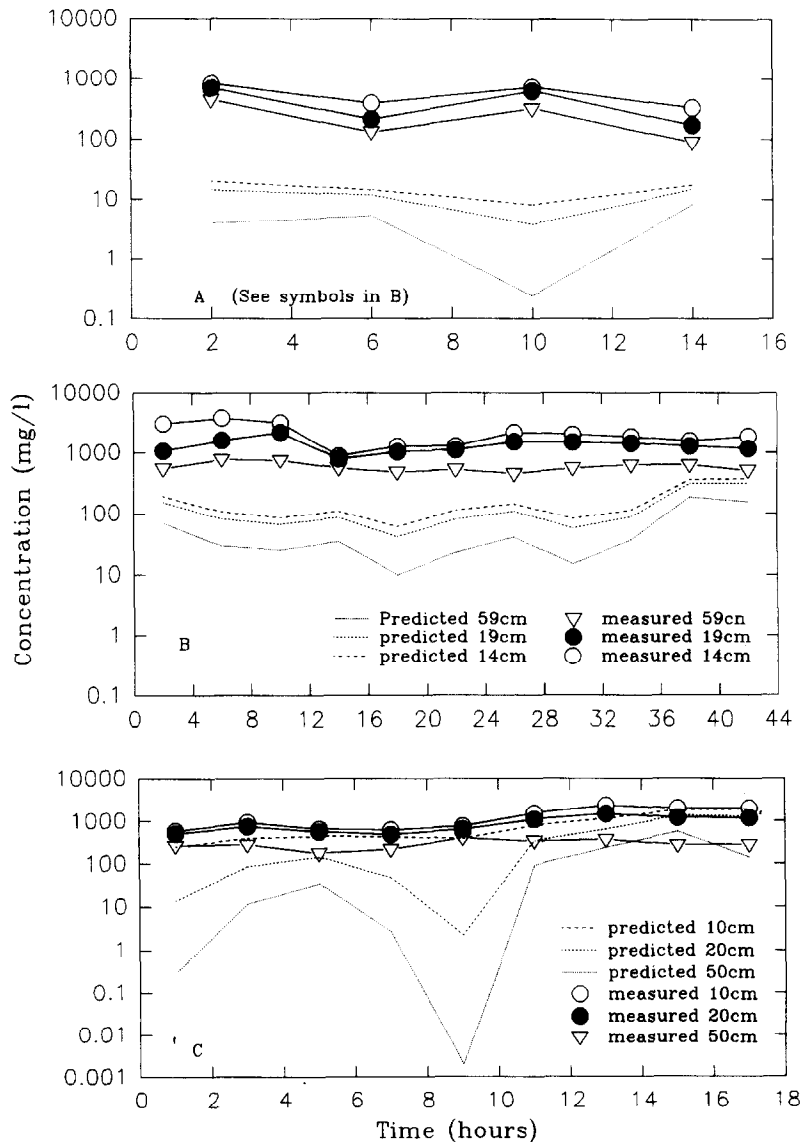


Fig. 11. Time series of measured and model-predicted suspended sediment concentrations at selected heights for (A) the 1985 fairweather period, (B) 1985 storm period and (C) 1988 experiment. Constant resuspension coefficient of 1.3×10^{-4} was used in the model prediction.

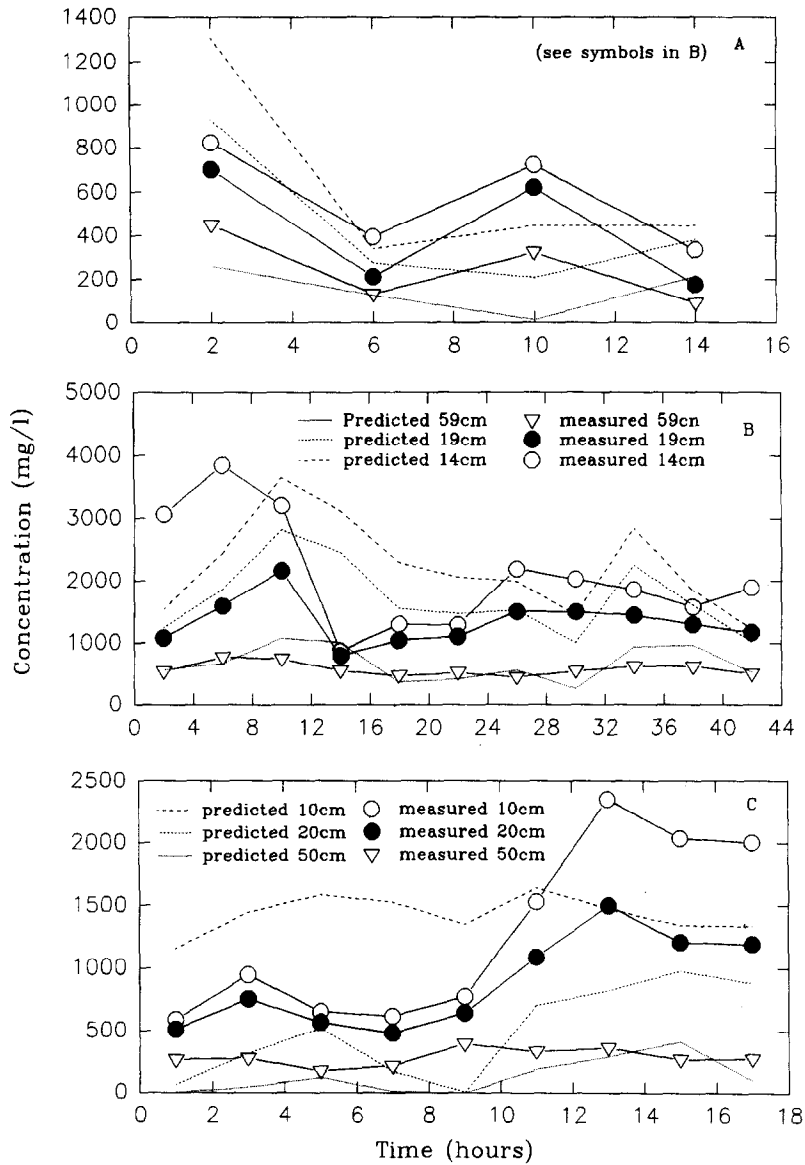


Fig. 12. Time series of measured and model-predicted suspended sediment concentrations at selected heights for (A) the 1985 fairweather period, (B) 1985 storm period and (C) 1988 experiment. Time variable resuspension coefficient was used in the model prediction.

Comparing Fig. 11 and Fig. 12 clearly shows that significant improvement is obtained in predicting suspension profiles by the use of a variable γ_0 : the model predicted sediment concentrations are generally within a factor of 2 from the measured concentrations and the variation trends are also in reasonable agreement. Close examination of

Fig. 12 shows that the predicted suspension peaks seem to lag behind the peaks of the measured sediment concentrations (e.g. hours 10 and 34 in Fig. 12B and hour 5 in Fig. 12C). These peaks generally correspond to the maximum ripple roughness shown in Fig. 4, indicating that the dependency of γ_0 on ripple roughness is probably over

weighted in the empirical Eq. 14 obtained through linear regression. The concentration at 10 cm height was not predicted well by the model for the 1988 experiment, but the predictions for 20 and 50 cm heights are better (Fig. 12C). Another striking characteristic is that when steady current shear velocity u_{*c} above the wave boundary layer is significantly lower than the corresponding settling velocity, the model tends to severely under-predict sediment concentrations for the upper heights, such as for hour 10 in Fig. 12A, hours 1, 3, 7 and 9 in Fig. 12C. In these cases, smaller settling velocities above the wave boundary layer (say $w_{s1} = u_{*c}$) or

complete bottom grain size distribution has to be used for better suspension profile predictions. The evaluation of the effects of mixed grain sizes on the computations of SSC is beyond the scope of this paper, but a good discussion can be found in Wiberg et al. (1994).

To better evaluate the suspension profile prediction by the Rouse equation, predicted and measured vertical SSC profiles are plotted in Fig. 13 for the 1985 fair-weather period, Fig. 14 for the 1985 storm period and Fig. 15 for the 1988 swell condition respectively. With a few exceptions, the model predicted suspended sediment concentration

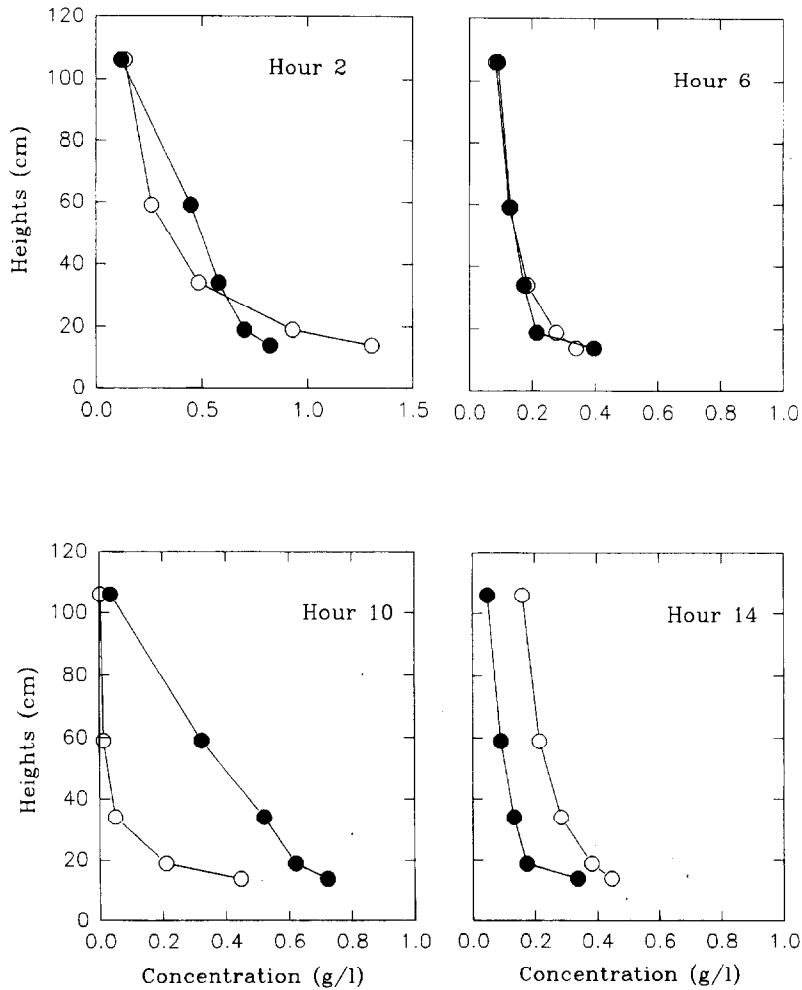


Fig. 13. Measured (dots) and model-predicted (circles) suspended sediment concentration profiles for the 1985 fairweather period.

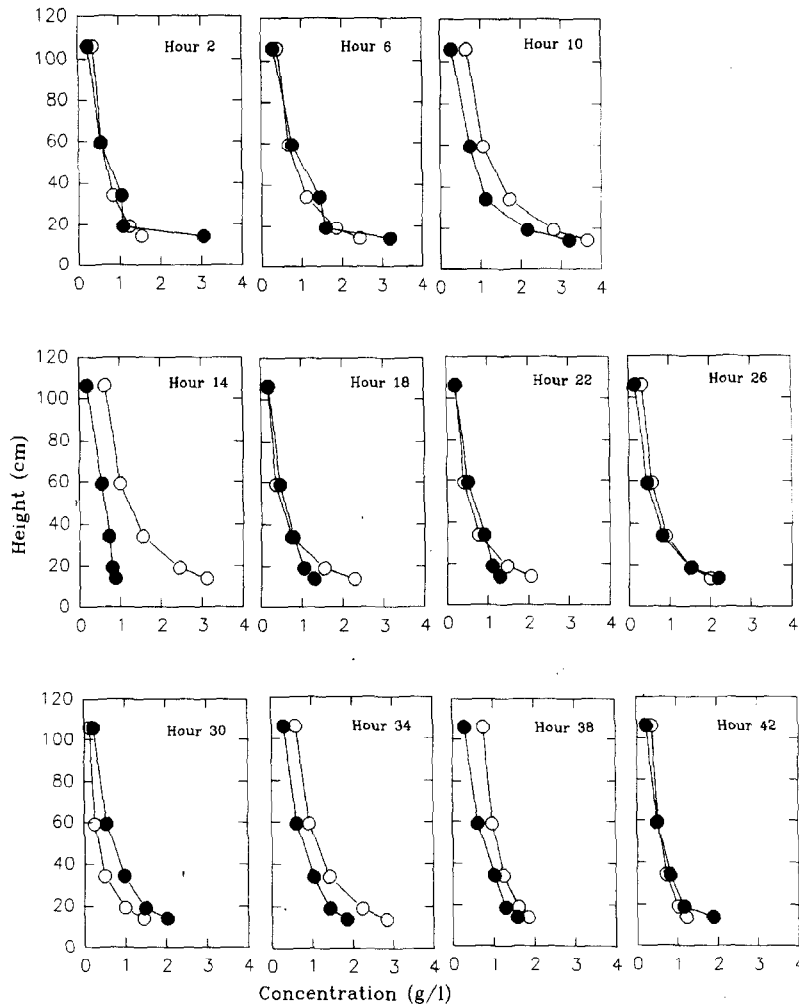


Fig. 14. Measured (dots) and model-predicted (circles) suspended sediment concentration profiles for the 1985 storm period.

profiles are in good agreement with the measured concentration profiles. The average difference, taken as predicted concentration minus measured concentration then divided by the measured concentration, is $\pm 62\%$ for the 1985 fair-weather experiment, $\pm 51\%$ for the 1985 storm period and $\pm 63\%$ for the 1988 swell experiment. These results are very encouraging given the fact that errors within an order of magnitude are often considered acceptable in predicting suspended sediment concentrations under combined flow field conditions. It is also interesting to see the close agreement in the exponential decay trend with height between the field measurements and model predictions.

This clearly suggests the general applicability of the modified Rouse equation given in Eq. 12 to the combined wave-current flows, provided that the BBL parameters and resuspension coefficient are correctly calculated.

In their field measurements of suspended sediment concentration profiles on shorefaces, Vincent and Green (1990) and Vincent et al. (1991) find that the GM model predicts a more uniform concentration gradient close to the bed than that shown by the measured profiles. They also find that the model-predicted wave boundary layers are too thick compared to that given by the measured concentration profiles for the low energy run

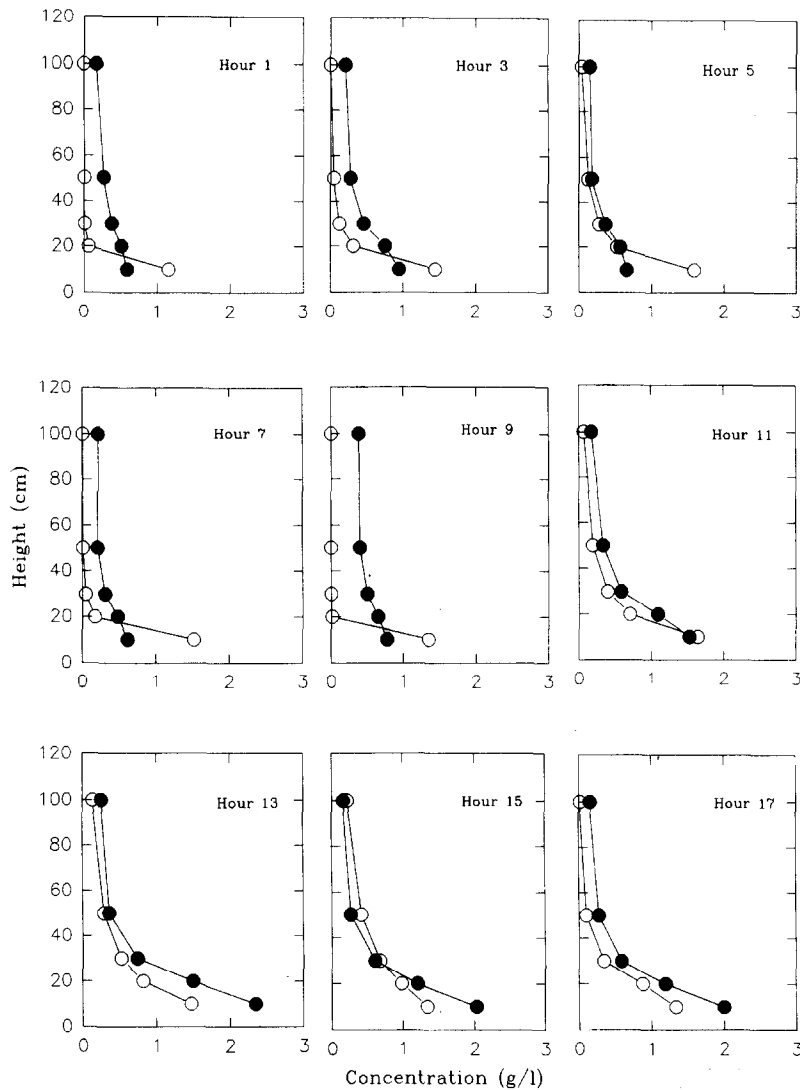


Fig. 15. Measured (dots) and model-predicted (circles) suspended sediment concentration profiles for the 1988 experiment.

(fig. 11 of Vincent et al., 1991). The lowest measured concentrations in the last four bursts of our 1988 experiment (hours 11 to 17 in Fig. 15) are within the wave boundary layer. The concentration gradient predicted by the model and wave boundary layer height indicated by this gradient change are in good agreement with that suggested by the measured concentration profiles. Vincent and co-workers have used the original ripple predictor of Grant and Madsen (1982), which generally overestimates ripple heights (Cacchione and

Drake, 1990) and thus the height of the wave boundary layer under low energy conditions. They also arbitrarily chose $z=2$ cm to calculate the reference concentration and resuspension coefficient. This has resulted in relatively smaller γ_0 compared to our study (see Fig. 10). The combination of smaller γ_0 and overestimated wave boundary layer height could explain the difference in concentration gradient and wave boundary layer height between their measurements and model predictions.

6. Discussions and conclusions

(1) The combined data of measured ripples from the Duck experiments and the Scotian shelf experiment suggest that the Grant and Madsen (1982) method overestimates ripple roughness for combined flow conditions, while the Nielsen (1981) method tends to under-predict ripple roughness. A modified ripple predictor (Eqs. 10 and 11) is proposed based on the Grant and Madsen method, and it is shown to give good predictions for the measured ripple roughness from the above mentioned field experiments. However, above conclusions and the general applicability of the proposed predictor await more high-quality field data for different grain sizes and wave-current flow conditions. For burst 9 in Fig. 6, an upper-flow regime flat bed resulted in zero ripple roughness, but the ripple predictor gave moderate ripple roughness. Thus it is important that a sheet flow criterion is included in a ripple predictor.

(2) Sand resuspension and reference concentration variation are controlled by the balance of near-bed skin friction shear stress and ripple development. Under low-energy fair-weather conditions, ripples are in equilibrium range and ripple roughness increases with the bed shear stress. This increased ripple roughness causes stronger vortex activity close to the bed and thus a higher resuspension coefficient γ_0 . Reference concentration c_0 can reach moderate values due to this ripple-enhanced resuspension, even though bed shear stresses are low (Fig. 7). Under high-energy storm conditions, the break off criterion is met and ripple roughness decreases with bed shear stress. This reduces vortex activity close to bed and sand resuspension coefficient is thus decreased. The combination of medium to high bed shear stresses and reduced yet still moderate ripple roughness leads to very effective sand resuspension, and reference concentrations are very high (Fig. 8). As bed shear stress is further increased, ripples are almost washed out and this minimum ripple roughness dramatically reduces sand resuspension and reference concentration reaches the lowest values despite the very high bed shear stresses (Fig. 9). When bed shear stress is increased beyond the sheet flow condition, resuspension coefficient and reference concen-

tration should increase with bed shear stress in theory. However, development of bed armouring layer and increased grain cohesion with sediment depth can limit these parameters to their minimum values. The upper plane bed Shields criterion under waves can be defined as $\theta_{up} = 0.413D^{-0.4}$, where grain size D is in millimeters (Komar and Miller, 1975). Based on this criterion, sheet flow occurred in the last two bursts of the 1988 experiment. Our estimated γ_0 and c_0 values shown in Fig. 9 seem to suggest relatively low reference concentrations and resuspension coefficients around 1.3×10^{-4} . This is in agreement with Hill et al. (1988), Vincent et al. (1991) and Madsen et al. (1993).

(3) When a constant γ_0 of 1.3×10^{-4} and modified Rouse equation are used to calculate suspended sediment concentration profiles, the predicted sediment concentrations are one to two orders of magnitude smaller than the measured concentrations. However, when a time variable resuspension coefficient together with the modified Grant and Madsen ripple predictor is used in the Rouse equation, the predicted suspended sediment concentrations are generally within a factor of 2 from the measured suspended sediment concentrations. These results suggest that sand resuspension coefficient γ_0 should not be a constant, but rather its value should increase with bed shear stress in the equilibrium range and decrease with bed shear stress in the break off range. The modified Rouse equation can be used to predict suspended sediment concentration profiles under combined wave-current flows, provided that the bottom boundary layer parameters and sand resuspension coefficient are correctly evaluated.

(4) When current shear velocity u_{*c} above the wave boundary layer is significantly lower than the median settling velocity of the bottom sediment, the model severely under-predicts suspended sediment concentrations at higher elevations. Ideally, after the ripple roughness and BBL parameters are properly evaluated, the complete bottom grain size distribution and lowest measured concentration should be used to obtain sand resuspension coefficient and predict the suspension profiles, instead of assuming constant settling velocities above and below the wave boundary layer. Complete grain size data were not available for

the 1985 and 1988 experiments. Total grain size distribution data were obtained in a 1992 field experiment. Though this was not from the bottom sediment samples of the 1985 and 1988 experiments, nevertheless it was used to recalculate γ_0 and this is then used to predict suspension profiles in Eq. 12. The overall agreement between the measured and predicted suspension profiles was slightly improved, but the improvement is not significant for those bursts in which u_{*c} is small. Our primary conclusion is that the modified Rouse equation does not properly predict suspended sediment concentration when u_{*c} is significantly smaller than the median settling velocity of the bottom sediment and that other factors such as horizontal advection or bed armouring should be examined. Fortunately smaller u_{*c} means smaller steady current velocities above the wave boundary layer so that this underestimate will not significantly affect the suspended sediment flux calculation.

Acknowledgements

The authors wish to thank John Boon and Jingping Xu of VIMS for their discussions during this work. We also like to acknowledge Donald Forbes and Steve Solomon of BIO, and an anonymous journal referee for reviewing the manuscript. This publication is Geological Survey of Canada Contribution No. 16494 and contribution number 1962 from the Virginia Institute of Marine Sciences.

References

- Adams, C.E. and Weatherly, G.L., 1981. Suspended-sediment transport and benthic boundary-layer dynamics. *Mar. Geol.*, 42: 1–18.
- Amos, C.L., Bowen, A.J., Huntley, D.A. and Lewis, C.F.M., 1988. Ripple generation under the combined influences of waves and currents on the Canadian continental shelf. *Cont. Shelf Res.*, 8: 1129–1153.
- Bagnold, R.A., 1946. Motion of waves in shallow water. Interaction between waves and sand bottoms. *Proc. R. Soc. London*, A187: 1–15.
- Birkemeier, W.A., DeWall, A.E., Gorbics, C.S. and Miller, H.C., 1981. A user's guide to CERC's Field Research Facility. U.S. Army Corps Eng., Coastal Eng. Res. Cent., MR 81–7.
- Businger, J.A., Wyngard, J.C., Izumi, Y. and Bradley, E.F., 1971. Flux profile relationships in the atmospheric surface layer. *J. Atmos. Sci.*, 28: 181–189.
- Cacchione, D.A. and Drake, D.E., 1982. Measurements of storm-generated bottom stresses on the continental shelf. *J. Geophys. Res.*, 87: 1952–1960.
- Cacchione, D.A. and Drake, D.E., 1990. Shelf sediment transport: an overview with applications to the Northern California continental shelf. In: B. Le Mehaute and D.M. Hanes (Editors), *The Sea*, 9. Wiley-Interscience, New York, pp. 729–773.
- Cacchione, D.A., Grant, W.D., Drake, D.E. and Glenn, S.M., 1987. Storm-dominated bottom boundary layer dynamics on the northern California continental shelf: Measurements and predictions. *J. Geophys. Res.*, 92: 1817–1827.
- Carstens, M.R., Neilson, R.M. and Altinbilek, H.D., 1969. Bedforms generated in the laboratory under oscillatory flow: analytical and experimental study. U.S. Army Corps Eng., Coastal Eng. Res. Cent., Tech. Mem., 28.
- Davies, A.G., Soulsby, R.L. and King, H.L., 1988. A numerical model of the combined wave and current bottom boundary layer. *J. Geophys. Res.*, 93: 491–508.
- Dingler, J.R., 1974. Wave formed ripples in nearshore sands. Ph.D thesis, University of California, San Diego, 136 pp.
- Drake, D.E. and Cacchione, D.A., 1989. Estimates of the suspended sediment reference concentration (C_a) and resuspension coefficient (γ) from near-bed observations on the California shelf. *Cont. Shelf Res.*, 9: 51–64.
- Glenn, S.M. and Grant, W.D., 1987. A suspended sediment stratification correction for combined wave and current flows. *J. Geophys. Res.*, 92: 8244–8264.
- Grant, W.D. and Madsen, O.S., 1979. Combined wave and current interaction with a rough bottom. *J. Geophys. Res.*, 84: 1797–1808.
- Grant, W.D. and Madsen, O.S., 1982. Moveable bed roughness in unsteady oscillatory flow. *J. Geophys. Res.*, 87: 469–481.
- Grant, W.D. and O.S. Madsen, 1986. The continental shelf bottom boundary layer. *Annu. Rev. Fluid Mech.*, 18: 265–305.
- Grant, W.D., Williams, A.J. and Glenn, S.M., 1984. Bottom stress estimates and their prediction on the northern California continental shelf during CODE-1: The importance of wave-current interaction. *J. Phys. Oceanogr.*, 14: 506–527.
- Hill, P.S., Nowell, A.R.M. and Jumars, P.A., 1988. Flume evaluation of the relationship between suspended sediment concentration and excess boundary shear stress. *J. Geophys. Res.*, 93: 12,499–12,509.
- Huntley, D.A. and Hazen, D.G., 1988. Seabed stresses in combined wave and steady flow conditions on the Nova Scotia continental shelf: Field measurements and predictions. *J. Phys. Oceanogr.*, 18: 347–362.
- Inman, D.L., 1957. Wave-generated ripples in nearshore sands. Tech. Memo 100, Beach Erosion Board.
- Kachel, N. and Smith, J.D., 1986. Geological impact of sediment transporting events on the Wahsington continental

- shelf. In: R.J. Knight and J.R. McLean (Editors), *Shelf Sands and Sandstones*. Can. Soc. Pet. Geol. Mem., II, pp. 145–162.
- Komar, P.D. and Miller, M.C., 1975. The initiation of oscillatory ripple marks and the development of plane-bed at high shear stresses under waves. *J. Sediment. Petrol.*, 45: 697–703.
- Li, M.Z., 1994. Direct skin friction measurements and stress partitioning over movable sand ripples. *J. Geophys. Res.*, 99: 791–799.
- Li, M.Z. and Amos, C.L., 1995. SEDTRANS92: A sediment transport model for continental shelves. *Comput. Geosci.*, 21(4): 533–554.
- Li, M.Z., Amos, C.L. and Wright, L.D., 1993. Estimating ripple roughness and sand resuspension coefficient γ_0 under combined flows: data from Scotian Shelf and Middle Atlantic Bight. *Proc. Euromech 310*. (Le Havre, France, September 13–17.)
- Madsen, O.S., Wright, L.D., Boon, J.D. and Chisholm, T.A., 1993. Wind stress, bed roughness and sediment suspension on the inner shelf during an extreme storm event. *Cont. Shelf Res.*, 13: 1303–1324.
- McCave, I.N., 1973. Some boundary-layer characteristics of tidal currents bearing sand in suspension. *Mem. Soc. R. Sci. Liege*, 6: 107–126.
- Miller, M.C. and Komar, P.D., 1980a. Oscillation sand ripples generated by laboratory apparatus. *J. Sediment. Petrol.*, 50: 173–182.
- Miller, M.C. and Komar, P.D., 1980b. A field investigation of the relationship between oscillation ripple spacing and the near-bottom water orbital motion. *J. Sediment. Petrol.*, 50: 183–191.
- Mogridge, G.R. and Kamphuis, J.W., 1972. Experiments on bed-form generation by wave action. *Proc. 13th Coastal Eng. Conf. ASCE*, Vancouver, pp. 1123–1142.
- Nielsen, P., 1981. Dynamics and geometry of wave-generated ripples. *J. Geophys. Res.*, 86: 6467–6472.
- Nielsen, P., 1984. Field measurements of time-averaged suspended sediment concentrations under waves. *Coastal Eng.*, 8: 51–72.
- Rouse, H., 1937. Modern conceptions of the mechanics of turbulence. *Trans. Am. Soc. Civ. Eng.*, 102.
- Smith, J.D., 1977. Modelling of sediment transport on continental shelves. In: E.D. Goldberg et al. (Editors), *The Sea*, 6. Wiley-Interscience, New York, pp. 539–577.
- Smith, J.D. and McLean, S.R., 1977. Boundary layer adjustments to bottom topography and suspended sediments. In: J.C.J. Nihoul (Editor), *Bottom Turbulence*. Elsevier, New York, pp. 123–151.
- Sternberg, R.W., Cacchione, D.A., Drake, D.E. and Kranck, K., 1986. Suspended sediment transport in an estuarine tidal channel in San Francisco Bay, California. *Mar. Geol.*, 71: 237–258.
- Vincent, C.E. and Downing, A., 1994. Variability of suspended sand concentrations, transport and eddy diffusivity under non-breaking waves on the shoreface. *Cont. Shelf Res.*, 14: 223–250.
- Vincent, C.E. and Green, M.O., 1990. Field measurements of the suspended sand concentration profiles and fluxes, and of the resuspension coefficient over a rippled bed. *J. Geophys. Res.*, 95: 15,591–15,601.
- Vincent, C.E., Young, R.A. and Swift, D.J.P., 1982. On the relationship between bedload and suspended load transport on the inner shelf, Long Island, New York. *J. Geophys. Res.*, 87: 4163–4170.
- Vincent, C.E., Hanes, D.M. and Bowen, A.J., 1991. Acoustic measurements of suspended sand on the shoreface and the control of concentration by bed roughness. *Mar. Geol.*, 96: 1–18.
- Wiberg, P.L. and Harris, C.K., 1994. Ripple geometry in wave-dominated environments. *J. Geophys. Res.*, 99: 775–789.
- Wiberg, P.L. and Nelson, J.M., 1992. Unidirectional flow over asymmetric and symmetric ripples. *J. Geophys. Res.*, 97: 12,745–12,761.
- Wiberg, P.L. and Smith, J.D., 1983. A comparison of field data and theoretical models for wave-current interactions at the bed on the continental shelf. *Cont. Shelf Res.*, 2: 147–162.
- Wiberg, P.L., Drake, D.E. and Cacchione, D.A., 1994. Sediment resuspension and bed armouring during high bottom stress events on the northern California inner continental shelf: measurements and predictions. *Cont. Shelf Res.*, 14(10/11): 1191–1219.
- Wright, L.D., Boon, J.D., Green, M.O. and List, J.H., 1986. Response of the mid-shoreface of the southern mid-Atlantic Bight to a “Northeaster”. *Geo-Mar. Lett.*, 6: 153–160.
- Wright, L.D., Boon, J.D., Kim, S.C. and List, J.H., 1991. Modes of cross-shore sediment transport on the shoreface of the Middle Atlantic Bight. *Mar. Geol.*, 96: 19–51.